

Article

Investigating the Potential for Increased Energy Utilisation and Reduced CO₂ Emissions at Mo Industrial Park

Torbjørn Pettersen ¹, Emil Dæhlin ² , Per Anders Eidem ²  and Olaf Trygve Berglihn ^{1,*} 

¹ SINTEF Industry, Process Technology, Postboks 4760 Torgarden, N-7465 Trondheim, Norway; torbjorn.pettersen@sintef.no

² SINTEF Helgeland, Postboks 1364, 8602 Mo I Rana, Nordland, Norway; emil.daehlin@sintef.no (E.D.); per.a.eidem@sintef.no (P.A.E.)

* Correspondence: olaf.trygve.berglihn@sintef.no

Received: 17 June 2020; Accepted: 31 August 2020; Published: 5 September 2020



Abstract: The potential for increased energy utilisation and reduced carbon footprint has been investigated for the industrial park Mo Industri Park (MIP), located at Mo i Rana, Norway. Process data has been gathered to quantify the energy flows between industrial clients. The energy flows have been visualised quantitatively in Sankey diagrams, while the quality of the available energy is presented in the form of a grand composite curve. High temperature flue gas from ferrosilicon (FeSi) production at Elkem Rana represent the largest heat source available for utilisation. A theoretical assessment of potential applications for this energy is presented and includes: (1) electricity production; (2) local biocarbon production, where surplus heat is utilised for drying of wood chips; (3) post combustion carbon capture, where surplus heat is utilised for solvent regeneration. The results indicate that increasing the current energy recovery from 400 GWh to >640 GWh is realistic. The increase in energy recovery can be used for reducing the carbon footprint of the industrial park. Investment in a common utility network for surplus heat may lower the threshold for establishing other energy clients at MIP. These are possibilities which may be investigated in more detail in future work.

Keywords: industrial parks; energy utilisation; CO₂ footprint

1. Introduction

The industry sector is directly emitting 24% (8.5 Gt) of total global CO₂ emissions and is accountable for 37% (156 EJ) of the global energy use [1]. Increased attention has been given to how interactions among different companies, industries and sectors can contribute to lowering the industry sectors' energy use and greenhouse gas emissions [2]. Such interactions are often seen within the scope of the circular economy and are usually divided into three levels: the micro level (products, companies, consumers), meso level (eco-industrial parks) and macro level (city, region, nation and beyond) [3]. At the meso-level, eco-industrial parks have gained increased attention in the last decades, and this is also labelled industrial symbiosis [4]. Geographic proximity and collaboration can provide and enable both economic and environmental benefits for the companies through the exchange of energy, water, materials, as well as services such as permitting transportation and marketing [4]. Several recent studies have highlighted how an energy-intensive industry located in industrial parks can gain increased energy and material efficiency as well as CO₂-reduced emissions through such symbiosis [5–9].

There is a vast literature in the field of industrial parks and their energy systems. Directions in research ranges from strategies and policies for development of eco-industrial parks [10,11], studies investigating how to measure the environmental performance [12,13], and optimisation of energy systems in industrial parks [14,15]. Energy recovery in industrial parks is a topic which has received

interest in the academic community and a number of systematic design techniques have been developed and applied over the years [16]. Total site heat integration (TSHI) was introduced by [17]. They extend the design and targeting procedures from Pinch Technology [18] to the concept of total sites, which constitute factories which are energetically linked through a central utility system. The methodology presented is applicable both in so-called grassroots design of new factories and in retrofit situations in existing factories and industrial sites. The methodology and relevant tools are further developed by [19], who reports results from a number of case studies where the applications of the methodology have resulted in savings in both energy (30%) and capital (10%). Matsuda et al. [20] presents results from applying area-wide pinch technology on one of the largest chemical complexes in Japan. The study demonstrated significant potential for energy savings at the site. The results were reported to have initiated several projects on energy recovery, where the total annual energy saving was estimated to around 250 GWh. Hackl et al. [21] performed a total site analysis (TSA) on the industrial cluster of chemical companies located in Stenungsund in Sweden. The report published in 2010 was meant to provide a basis for future implementation of energy system integration. The following methodology was applied:

- Stream data for temperature and enthalpy flows (T_{Start} , T_{end} , Q) and data on utility consumption was collected.
- Steam from by-product incineration was also considered as a source for process heat.
- The data was presented in so-called total site profiles (TSP) and total site composite curves (TSC). This analysis provided information on the site pinch temperature and was used to identify the most attractive measures to increase heat recovery.
- The sitewide potential for co-generation and measure for reducing the external cooling demand below ambient temperature was also analysed.

Røyne et al. [6] revisited the Stenungsund chemical industry cluster and compared the current state of an industrial park with possible future configurations focusing on increased energy integration and replacing fossil feedstock with forest-based feedstock and compared the different scenarios in a lifecycle assessment. According to [6], little attention has been given to analyse how the environmental impact can be further reduced in already existing industrial parks. An investigation of how environmental impact can be reduced in existing parks is case-specific in its nature, and the approach used in this study will therefore use a case study as a basis.

Mo Industrial Park (MIP) at Mo i Rana is one of Norway's largest industrial parks. The park hosts ferroalloy and steel industries together with several other industrial companies. The ferroalloy and steel industry is characterised as an energy intensive industry with large demands for electrical energy in particular. A large surplus of thermal energy is generated by the process and is available over a wide range of temperature levels. MIP has for a long time recognised the surplus energy as a valuable asset for the industrial park and has, together with the industrial clients, been working ambitiously with energy recovery. Currently, MIP is reporting an annual energy recovery of 400 GWh out of an estimated potential of 900 GWh (Figure 1). Their ambition is to increase the annual energy recovery to 640 GWh by further utilising available energy streams.

The aim of the current study is to gather data on the current energy use within the park and evaluate theoretically the potential for alternative utilisation of the surplus energy in applications which may be beneficial to the current industrial clients. The industry has identified the replacement of fossil carbon reduction materials with increased use of bio-based reduction material (biocarbon) and CO₂ capture and utilization or sequestration as the applications of greatest potential. The heat integration potential with future carbon capture facilities and biocarbon production facilities will therefore be explored theoretically.

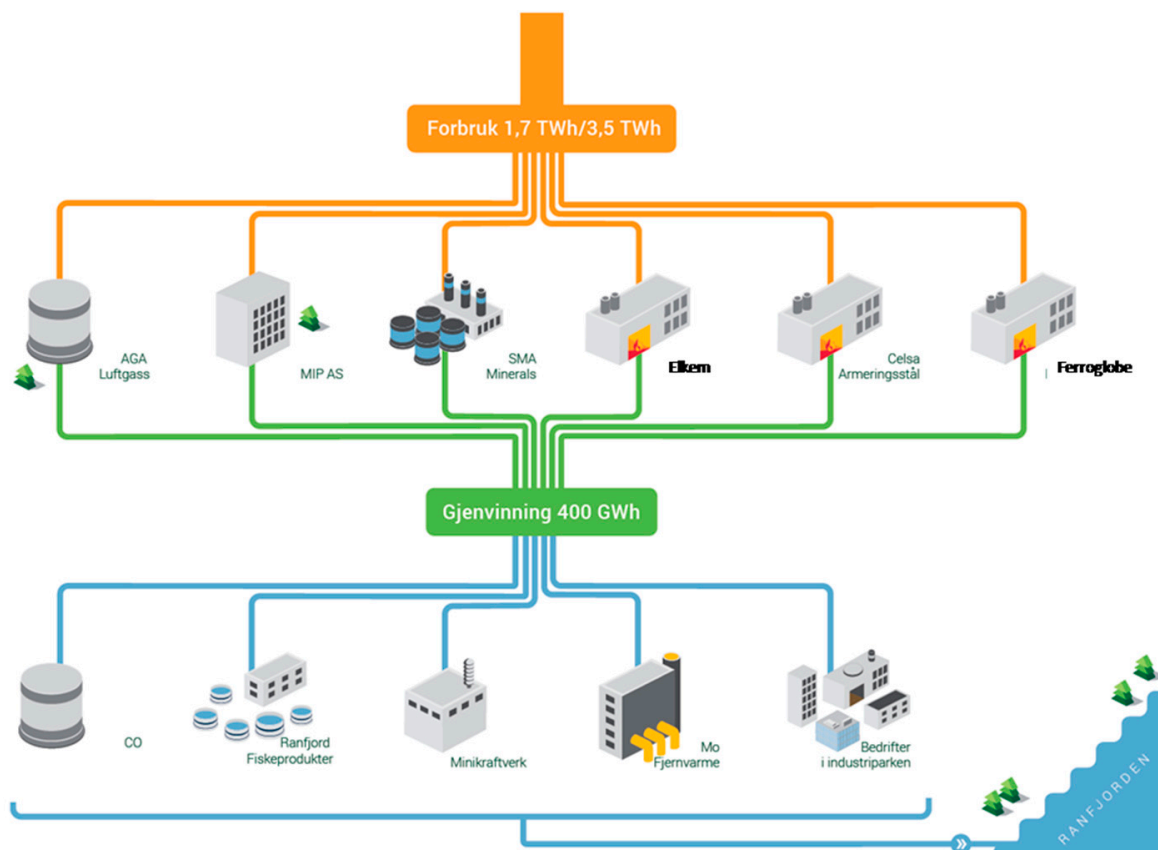


Figure 1. Energy recovery at Mo Industrial Park (adapted from MIP Magasinet 2016).

2. Methodology

In order to assess the energy use and potential for recovery, a mapping of the current energy flows and temperature levels was required to establish a reference base case. This is a challenging task as it involves multiple industrial entities, the production can have seasonal variations with changing ambient conditions, not all states and magnitudes of process flows are measured or easily estimated, etc. In this work, the industrial entities are treated as independent units and only the known exchanges over the company battery limits were considered. The exchanges are either raw materials that represent significant energy content, utility exchanges, or products and effluents.

Data has been systematically gathered for all major entities in the industrial park in order to evaluate the current status and future potentials for energy use. This data serves as a parameter set for modelling the total energy flow and establishing a benchmark. Some prospective new processes are considered and the effect of the integration on the total energy flow is analysed.

2.1. Data Collection and Analysis

More than 100 different companies are located in Mo Industrial Park. The focus in this analysis is the process industry. Other actors in the park are considered relevant if they are either (1) large energy consumers or (2) interlinked with the process industry in terms of energy flows. Based on this, the actors listed in Table 1 were identified:

Table 1. Relevant actors and key infrastructure in Mo Industrial Park.

Actor/infrastructure	Explanation
Elkem Rana	Ferrosilicon
Ferroglobe Mangan	Silicomanganese and ferromanganese
Celsa	Reinforcing steel (from steel scrap)
SMA Minerals	Quicklime and calcined dolomite
Ranfjord fiskeprodukter	Land-based aquaculture
Aga	Industrial gases (cryogenic)
Bitfury	Data centre
MIP AS	Utility and property company
Syn-gas grid	CO-rich gas from Ferroglobe is utilised in other companies
Mo Fjernvarme	District heating from recovered surplus heat
Cooling water	Flow-through from nearby reservoirs

The collected data was compiled from a combination of publicly available sources and from data provided by the respective companies. The publicly available data has been used wherever possible and complemented by calculations and approximations based on the literature. The collected energy data was confined to the geographical co-located industrial companies in MIP at the companies' battery limits, see Figure 2.

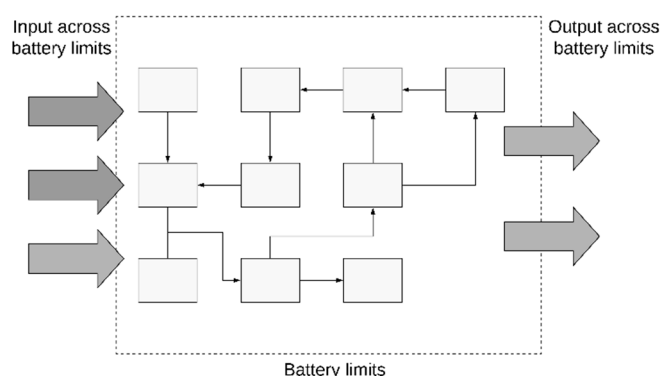


Figure 2. Illustration of battery limits for an industrial company at Mo Industrial Park (MIP). Only flows across the battery limits of companies are considered in this analysis.

The annual energy input was found using official statistics for the companies which are subject to the Norwegian Environment Agency's reporting obligation and Pollutant Release and Transfer Register (PRTR) [22]. The electricity demand is given in MWh while consumption of fossil fuels, reduction agents, etc. are given in tonnes. The energy content was found by assuming calorific values for the different energy inputs as given in Table A4 in Appendix B.1.

The energy inputs were aggregated into the categories of electricity, coal/char/coke, oil products, gas and biocarbon to simplify the analysis. This energy is consumed and used in reduction processes or for heating purposes and by that converted to chemical or thermal energy. Data on the chemically bound energy and surplus heat were estimated by using open references. Energy assessments from literature were used as estimates for the local cases to allocate surplus heat to the different energy streams. Energy balances were established to reveal lacking information and ensure energy balance consistency. Inconsistencies in energy balances were assigned to energy losses, and thus close the balance.

Figure 3 illustrates the energy flows across the battery limits for the selected actors (listed in Table 1) as a Sankey diagram. The main input is electricity and coal/char/coke which is used as a chemical reduction medium for metal oxides in the submerged arch furnaces (SAF) operated by Elkem and Ferroglobe. The data centre operated by BitFury is also a significant electricity consumer. In Figure 3, the most significant energy integration is carried out by:

1. “MIP CO nettverk” which redistributes carbon monoxide (CO)-rich flue gas (204 GWh) from Ferroglobe for heating purposes at Celsa, SMA Minerals, and Mo Fjernvarme
2. “Mo Fjernvarme” which recovers latent heat from flue gas from Elkem (125 GWh) for use as district heating
3. “Ranfjord fiskeprodukter” which utilises cooling water from Elkem (40 GWh).

In total, this sums up to 369 GWh of recovered energy. In addition to the abovementioned utilisations of surplus heat, MIP also produces electricity from turbines in the water-cooling utility systems. This is not shown in the Sankey diagram in Figure 3, as the focus in this work is the surplus heat.

While Figure 3 illustrates the size of energy flows between the various actors, it does not provide information on the possibilities for further heat integration, which among other things depends on the temperature level of the heating and cooling demands. This information can be illustrated in a so-called Grand Composite Curve (or Heat Surplus Diagram) [18,23] which shows the aggregated heating and cooling demands at each temperature level of the process streams. The Grand Composite Curve for MIP in Figure 4 shows that MIP has an energy surplus. The existence of pockets in the curve, such as in the case for temperatures less than 80 °C in the right end of the curve, indicates a possibility for heat integration between an enthalpy surplus and an enthalpy demand. Except for the low temperature end, the remainder of the curve shows no such significant pockets. There is no heating demand above the process pinch temperature (at 1200 °C). The energy available at the temperature interval 1200–600 °C is related to cooling of metal from the SAF. Although studies have been made [24], this energy is likely to be more challenging to utilise compared to the energy available in flue gas from Elkem (below 600 °C). In the Sankey diagram in Figure 3, this flue gas stream has been split into “Off gas, unavoidable heat loss” which represents the energy in the flue gas in the temperature interval from ambient to 180 °C. Due to local environmental considerations, governmental regulations are imposed on the lower limit of flue gas emissions. The energy stream to “Off gas pipe loss” (332 GWh) represents the energy content in flue gas in the temperature interval 600–180 °C which could be utilised.

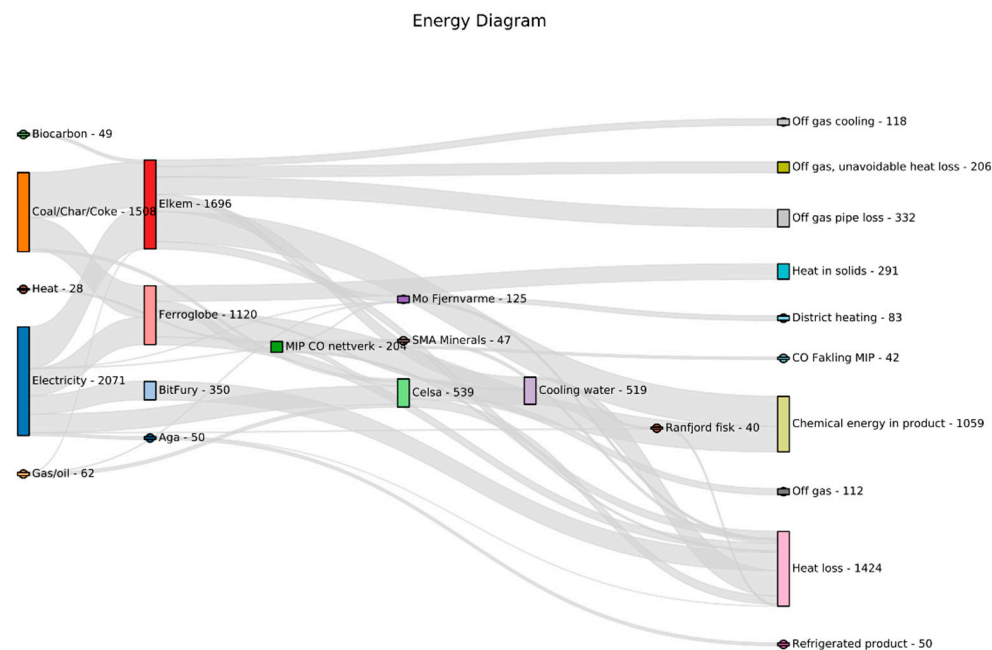


Figure 3. Sankey diagram for annual energy flows (GWh). See Table A3 in Appendix A for aggregated energy flow data across battery limits at Mo Industrial Park.

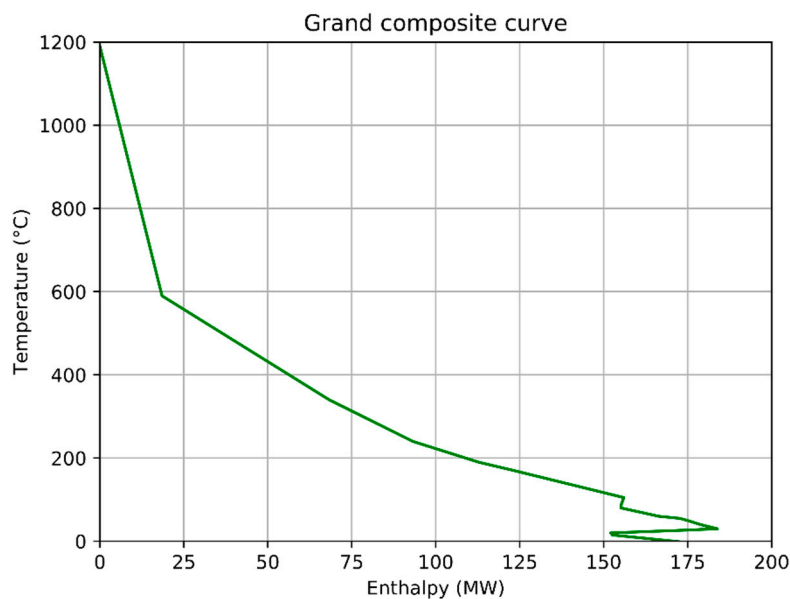


Figure 4. Grand composite curve for selected streams (gas, liquids, solids) between energy actors within MIP. See Appendix B.1 Table A4 for detailed stream data.

A significant high quality/temperature energy source available for utilisation can be identified from Figure 4. Above 200 °C, the available thermal effect is around 100 MW. Of these, about 40 MW is available as continuously produced flue gas at a temperature level of 180–600 °C. The main challenge is to identify existing or new energy consumers that can utilise the surplus energy in a sustainable and economical way.

2.2. Modelling

A simplistic modelling approach has been applied to describe the overall mass and energy flows between the industrial processes included in this work. The purpose has been to describe qualitatively the main design tradeoffs which are being investigated. A complete description and modelling of all industrial actors within MIP is outside the scope of this work. With respect to cost estimation, the focus has been on cost related to electricity consumption and cost related to the CO₂ emissions. Other energy input costs, such as the cost for biocarbon and the coal it replaces, have been omitted in this study. Capital expenses related to proposed design changes have not been included.

2.2.1. Silicon and Ferrosilicon Production

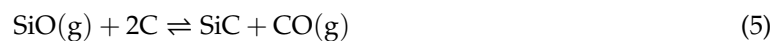
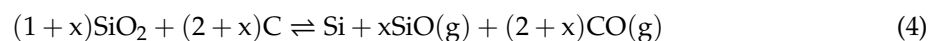
In the following, an overview will be given of the Silicon (Si) and Ferrosilicon (FeSi) processes. This is based on Schei et al. [25] and Tangstad [26], and further details may be found there. Elkem Rana produces FeSi in two submerged arc furnaces with a total electrical power of above 100 MW.

The Si and FeSi processes are both performed in open and semi-closed furnaces, meaning that air is supplied to the charge top of the furnace to oxidize CO(g) and SiO(g) according to Equations (1) and (2). The electrical power is supplied through three Søderberg electrodes of typically 1.4–1.9 m in diameter.



The furnaces may be charged by batch charging, but, from an environmental point of view, it is beneficial with a semi-continuous charging [27]. This is due to an increased flue-gas temperature that destroys polycyclic aromatic hydrocarbons (PAH) and dioxins. The main components of the charge

mix are quartz, carbon material (charcoal and/or coal), in some cases wood chips, and for FeSi, an iron source such as iron ore pellets. Electric energy is supplied through three electrodes that are submerged in the charge. The furnace process may roughly be divided into a hot zone and a colder zone, where the latter is the upper part of the furnace and the former is the lower part of the furnace centred around a crater where an electric arc dissipates energy. The overall reaction of the furnace may be given as in Equation (3). Equation (4) describes the reaction taking place in the hot part of the furnace, where Si(l) and SiO(g) is formed. Further, SiO(g) from the hot zone will be a loss of Si units if not either reacted with carbon (Equation (5)) or condensed (Equation (6) or (7)) in the colder zone of the furnace.



In the later years it is common at Norwegian Si and FeSi plants to have energy recovery. At Elkem Rana there is currently a boiler installed to recover heat for the district heating system at Mo i Rana, the largest based on recovered energy in Norway.

The flue gas composition and flow rate from a FeSi SAF has been described based on parameters outlined in Table 2 and represent typical average flue gas composition from a FeSi furnace. The composition will vary some based on operating conditions and charge composition. Typically, the moisture content increases during the winter due to ice and snow in the raw materials. It represents a simplistic modelling approach which can be representative for a “generic” quality of FeSi. A description of the energy flow around the furnace is given here, which will give a qualitatively correct representation. The composition of the flue gas from the charge top is specified and is based on information from the project Staged Combustion for Energy Recovery in Ferroalloy industry (SCORE) [28,29]. The flue gas flow rate is assumed to scale linearly with the furnace electrical power. The same applies for mass flows of ore, carbon and metal produced [30–32]. The mass and energy balances for combustion of furnace flue gas with air and recirculated flue gas are calculated using the open source physical properties library [33], which is based on the Shomate enthalpy correlations from the National Institute of Standards and Technology (NIST) Chemistry WebBook [34,35]. Recirculated flue gas is used to meet the maximum inlet temperature (750 °C) to the waste heat recovery unit (WHRU) in cases where the amount of excess combustion air (ingress air) alone would not be sufficient to cool down the flue gas before the waste heat recovery unit. The simulation of the SAF performance was based on the parameters given in Table 2.

Table 2. Ferrosilicon production base case parameters.

Parameter	Value
Charge gas composition (vol.%)	CH ₄ : 9, CO: 57.6, SiO: 3.7, H ₂ : 6.4, H ₂ O: 23.3, N ₂ : rest
Charge gas temperature	1500 °C
Specific charge gas generation	287.5 Nm ³ /(h*MW)
Specific electricity consumption	11.7 MWh/t Me
Specific carbon consumption	1.7 kg/kg Me
Max inlet temperature to WHRU	750 °C
Recirculated flue gas temperature from WHRU	150 °C
Heat loss from SAF	1500 kW

2.2.2. Waste Heat Recovery Unit

The waste heat recovery unit was simulated with design parameters as given in Table 3. For external energy clients, it was assumed that the thermal energy was taken out as saturated steam. The flue gas from the SAF was assumed to have a maximum temperature of 750 °C. The physical properties of water and steam were calculated using the open source implementation of the international-standard IAPWS-IF97 steam tables [36].

Table 3. Design parameters for waste heat recovery unit with steam turbine for electricity production.

Design Parameter	Value
Flue gas inlet-outlet temperature (°C)	750–150
Flue gas heat loss (%)	2
Steam pressure (bar)	40
Superheated steam temperature (°C)	420
Saturated steam temperature (°C)	250
Steam turbine isentropic efficiency (%)	75
Turbine exit temperature and pressure (°C), (bar)	45.8, 0.1
Generator overall efficiency (%)	98

2.2.3. Carbon Capture

Conventional amine-based absorption technology for post combustion CO₂ capture has been considered in this work. At MIP there are several potential flue gas sources which are candidates for a carbon capture facility, where either use or storage of CO₂ is possible. For absorption-based CO₂ capture, the main energy requirements are linked to thermal regeneration of the amine solvent which takes place in a stripper column typically operating at a reboiler temperature of around 120–130 °C. Once the solvent system has been selected, the thermal energy requirements are defined by the specific reboiler duty (SRD) (GJ/t CO₂), which is a function of the CO₂ concentration in the flue gas [37] and of the capture rate.

The specific reboiler duty for state-of-the-art absorption technology has been demonstrated by using 30 wt% mono ethanol amine (MEA) as solvent at the Norwegian test facility TCM [38]. Gorset et al. [39] reports that the specific reboiler duty of 3.8 MJ/t CO₂ captured was achieved with MEA as a solvent operating at 87% capture rate on a flue gas with 3.7 vol% CO₂.

The influence on energy consumption and the concentration and capture rate has been investigated theoretically by [40]. They derived the following theoretical relation for the ideal work of mixing of CO₂ as a function of flue gas concentration and CO₂ capture rate:

$$W_{Mix} = -\frac{RT}{n_C M_{CO_2}} \left(\ln \frac{1}{y_{CO_2}} + \frac{1 - n_C y_{CO_2}}{y_{CO_2}} \ln \frac{1}{1 - n_C y_{CO_2}} + (1 - n_C) \ln (1 - n_C) y_{CO_2} - n_C \ln p_r \right) \quad (8)$$

By normalising with the results reported by for MEA, we get a rough estimate for the SRD as a function capture rate and flue gas composition as follows:

$$SRD(n_C, y_{CO_2}) = 3.8 \text{ MJ/t CO}_2 \frac{W_{Mix}(n_C, y_{CO_2})}{W_{Mix}(n_C = 0.87, y_{CO_2} = 0.037)} \quad (9)$$

Figure 5 shows the estimated specific reboiler duty for a range of conditions when estimated using Equation (9). It is expected that the estimated SRD is too low for high concentrations of CO₂. However, the qualitative trend can be expected to be correct and the accuracy to be sufficient at this conceptual level of design. Knudsen et al. [41] tested three different solvents (20 wt% MEA, CESAR1 and CESAR2) on flue gas from a coal power plant (13 vol% CO₂). The best solvent (CESAR1) achieved an SRD value close to the 90% capture line in Figure 5.

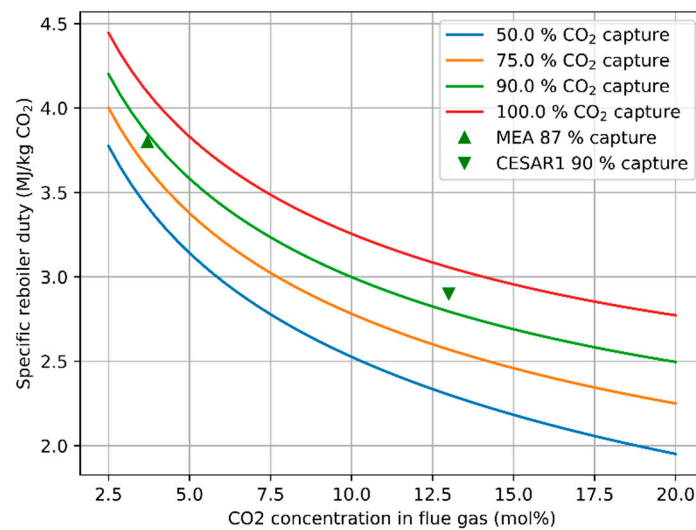


Figure 5. Estimated specific reboiler duty for a generic solvent as a function of CO₂ capture rate and flue gas concentration. Based on theoretical work of mixing [40] and normalised with results for 30 wt% MEA [39]. The performance of the CESAR1 solvent (90% capture rate, 13 vol% CO₂) [41].

2.2.4. Biocarbon Production

The modelling framework and assumptions made regarding biocarbon production was to a large extent based on the work by Olszewski et al. [42]. They present a techno economical evaluation of biocarbon production processes, with focus on Norwegian conditions and conclude that there are economic benefits by supplying logwood rather than wood chips to the end user of biocarbon. We therefore consider production of biocarbon at the ferroalloy plant where surplus heat may be utilised for the energy intensive drying process of virgin biomass. The composition of produced biocarbon, pyrolysis gas and pyrolysis oil is estimated from empirical correlations presented in [43].

2.3. Key Performance Indicators

The key performance indicators used in this study are focusing on CO₂ footprint, net electricity consumption or costs related to both factors. The key performance indicators in this study are limited to a per company level, or on the battery limits of the production facility. The performance of the whole park was not assessed.

1. CO₂ footprint as kg CO₂ equivalents per kg metal produced (kgCO₂/kg Me)
2. Net electricity consumption as kWh(el) per kg metal produced (kWh/kg Me). Net electricity consumption is electricity input to SAF minus electricity produced in the waste heat recovery steam cycle
3. Electricity and CO₂ emission costs per kg metal produced (EUR/kg Me).

The parameters related to the key performance indicators are summarized in Table 4.

Table 4. Economic parameters related to key performance indicators. Base case figures are given in bold.

Parameter	Range	
Electricity price from grid	0.03–0.1	EUR/kWh
CO ₂ emission price	5–30	EUR/t CO ₂
CO ₂ emissions from electricity production	25–440	g CO ₂ -eq/kWh

The carbon footprint is analysed on two levels or scopes. Scope 1 include the direct CO₂ emissions from the combustion of fuels from the stationary processes within the industrial park. Scope 2 emissions include the indirect CO₂ emissions related to the consumed electricity in the industrial park.

Biogenic CO₂ emissions are regarded as CO₂ neutral in the CO₂ footprint. The biogenic CO₂ emissions will not contribute towards the CO₂ emission cost, in line with the regulatory framework EU Emissions Trading System (EU ETS).

The carbon emissions related to the consumption of electricity depend on regional attributes. The regional average production mix, along with imports from neighbouring regions, will yield different carbon intensities of CO₂/kWh depending on the regional scope. Several on-line statistics are available which can provide a snapshot of the CO₂ footprint per kWh electricity produced or consumed in a given region. The average carbon intensity for different regional scopes are Norwegian (30.5 g CO₂-eq/kWh, low-voltage mix) [44], Nordic electricity mix (130 g CO₂-eq/kWh) [45], and European (446 g CO₂-eq/kWh) [44]. An approximation for the Norwegian high voltage electricity mix was used as a baseline at 25 g CO₂-eq/kWh (the high voltage mix has a lower carbon intensity because of lower losses).

The CO₂ price in Europe has since 2008 and 2019 varied from 5 to 30 EUR/t CO₂. The highest prices were obtained prior to the financial crisis in 2008 and again in 2019 where prices approached 30 EUR/t CO₂. In the period after the financial crisis in 2008 and up until 2017, the CO₂ prices were 10 ± 5 EUR/t CO₂ [46]. A CO₂ price of 30 EUR/t was used as the baseline.

The price of electricity for non-household consumers varies in the range from 0.15 EUR/kWh (Germany) to about 0.07 EUR/kWh (Finland). Norway is listed with a price around 0.09 EUR/kWh [47]. These electricity prices for Norway are significantly higher than what Statistics Norway presents as electricity prices for energy intensive industry (0.3 NOK/kWh which is about 0.03 EUR/kWh) [48]. An electricity price at 0.03 EUR/kWh was used as baseline.

Figure 6 shows the fraction of the total electricity price which represents the CO₂ costs as a function of CO₂ generation caused by electricity production. For the Norwegian market with a low specific CO₂ production per kWh electricity, the CO₂ costs represent a small part of the total costs. However, if a European electricity mix is considered with almost 10 times higher specific CO₂ production per kWh, the cost of CO₂ becomes a significant fraction of the overall electricity cost.

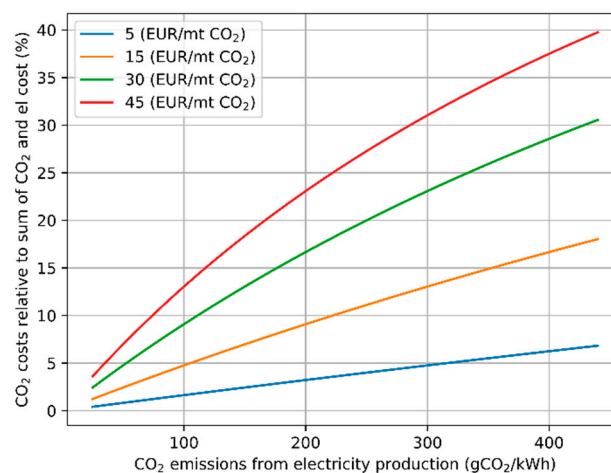


Figure 6. CO₂ cost relative to total cost of electricity assuming typical Norwegian electricity costs at 0.03 EUR/kWh.

Comparisons made on an energy basis have received criticism in that an energy quantity does not reflect the energy potential or thermodynamic “value” of a material [49]. For electricity where losses for voltage (potential) transformations is for the most case negligible, the electrical energy can be used directly in comparisons, irrespective of voltage. To quantify energy for mass flows in heat

exchange or involving heat of reactions and phase transformations, some reference must be made to the thermal, mechanical and chemical potential. A simplified analysis based on ambient reference can be made using the concept of exergy or potential useful work extraction [50]. The exergy accounts for the difference in value for work production of a given energy quantity available for two different temperatures. Still, this analysis suffers from the same problem of attributing a per unit product value when having multiple products and quantities.

For ease of comparison and for comprehensive communication of results, this work has focused on comparing the effect on the change in net electricity consumption when including CO₂ capture and biocarbon production, while attributing a quota cost for the emission of CO₂.

3. Potential New Energy Clients

The energy analysis for Mo Industrial Park shows that there is a significant energy surplus within the park. In the temperature range of 600–200 °C, surplus energy is accessible in the form of hot flue gas from the Elkem production. The default utilisation of this surplus heat would be waste of heat recovery with electricity production, which is currently installed at several ferroalloy production sites in Norway. However, electricity production gives an inherently low utilisation factor (typically <30% of the thermal energy is converted to electricity) and has high capital costs associated with waste heat recovery boilers for super-heated steam production and high-pressure steam turbines. Figure 7 illustrates a number of alternative processes which may utilise surplus thermal heat directly as saturated steam from a more inexpensive waste heat recovery system.

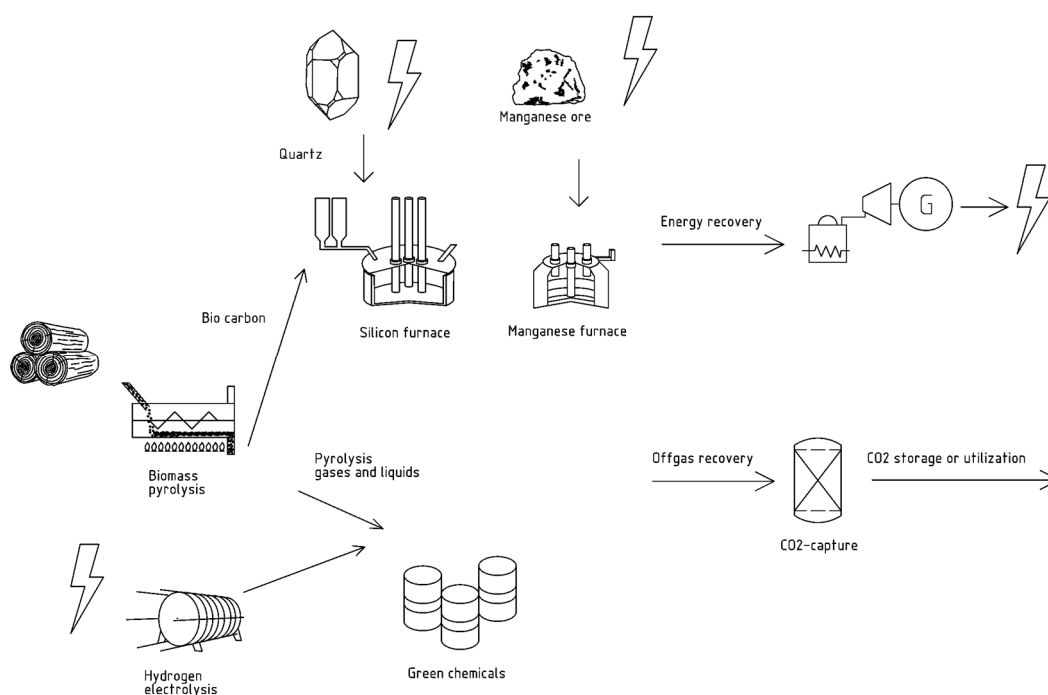


Figure 7. Opportunities for energy integration between ferroalloy production and other sustainable production processes.

In the following theoretical evaluations, we have focused on two energy demanding production activities which are closely related to improving the sustainability of ferroalloy production processes by reducing the carbon footprint in the processes. Both biocarbon production and post combustion carbon capture represents value chains which are common to both ferro alloy producers at MIP. Both production processes are energy intensive operations which are able to utilise surplus heat in the temperature range around 200 °C. The energy consumption for carbon capture is linked to the CO₂

concentration in the flue gas. A simple evaluation of the effect of using recirculated flue gas for flue gas temperature control is therefore included.

In terms of robustness and energy integration between the two ferroalloy producers at MIP, local biocarbon production and carbon capture makes sense as the value chains are interconnected.

3.1. Ferrosilicon Production

The base case for ferrosilicon production was chosen as a 40 MW furnace with a waste heat recovery unit for electricity production. The furnace performance was estimated based on the parameters outlined in Table 2.

3.1.1. Semi-Closed Furnace with Recirculated Flue Gas

Currently, most silicon and ferrosilicon production in Norway is carried out using semi-closed furnace technology, where ingress air is used for controlled combustion of the charge gas being generated in the SAF. In order to maintain a stable flue gas temperature (650–750 °C) towards the waste heat recovery boiler, a high degree of ingress air is required. This leads to a dilute flue gas with high O₂ surplus and low CO₂ concentration. The large amounts of ingress air also lead to significant stack loss, since ingress air is heated from ambient temperature to the stack temperature of around 150 °C. Thus, the semi-closed furnace technology limits the amount of energy which can be recovered from the flue gas.

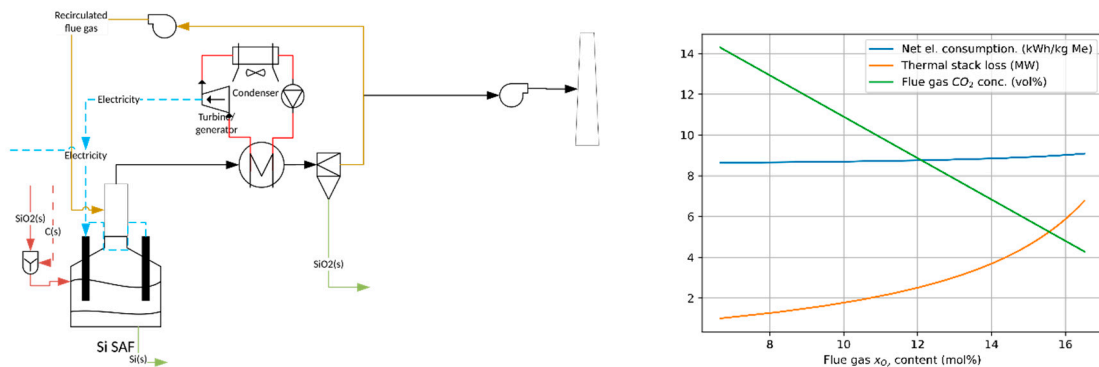
The ferrosilicon industry has been working on establishing a semi-closed furnace technology where the combustion of the charge flue gas takes place at a lower oxygen concentration. The recirculated flue gas (from downstream the waste heat recovery system) is used for temperature control in the flue gas entering the waste heat recovery boiler. A semi-closed furnace technology with recirculated flue gas will enable recovering more energy in addition to the possibility of avoiding peak temperatures in the combustion zone. Avoiding peak temperatures will also reduce the NO_x formation from the process (Wittgens et al. [28]).

Figure 8a illustrates a base case scenario for a generic ferrosilicon production, with a SAF integrated with a waste heat recovery boiler producing super-heated steam for electricity production in a Rankin steam cycle. The process flow diagram indicates how recirculated flue gas may be used for temperature control in the combustion zone and upstream of the waste heat recovery boiler. In a semi-closed furnace, the amount of ingress air can be limited to what is required for complete combustion of the flue gas. For such cases, recirculated flue gas can be used to control the flue gas temperature at the inlet of the waste heat recovery boiler below the target 750 °C. Figure 8b illustrates how reduced ingress air (reduced O₂ content in the flue gas) affects both the stack loss and leads to reduced net electricity consumption (5% reduction) as more thermal energy is available for steam production. The stack loss is reduced from close to 7 MW down to about 1 MW when ingress air for cooling the flue gas is replaced by recirculated flue gas. The carbon dioxide concentration in the flue gas increases from 4 to 14 vol% as we move towards a semi-closed furnace with recirculation of flue gas operating at 7 vol% O₂. An increase in CO₂ concentration will have a positive impact on the energy consumption in any downstream CO₂ capture processes.

3.1.2. Biocarbon Production

Replacement of fossil carbon (typically coal, char or coke) with more CO₂-neutral biocarbon (charcoal and some woodchips) has been an important research area over the last decades [42,51]. Local production of biocarbon from virgin biomass offers several obvious integration opportunities in terms of energy recovery. The main motivation for introducing biocarbon is to reduce the carbon footprint of the silicon production. The drying process of the biomass prior to pyrolysis/biocarbon production can operate using waste heat from the ferrosilicon production process and other surplus heat sources within MIP. Thus, enabling efficient use of surplus energy with a less capital intensive and more thermodynamically efficient process than electricity production. Although we focus here on

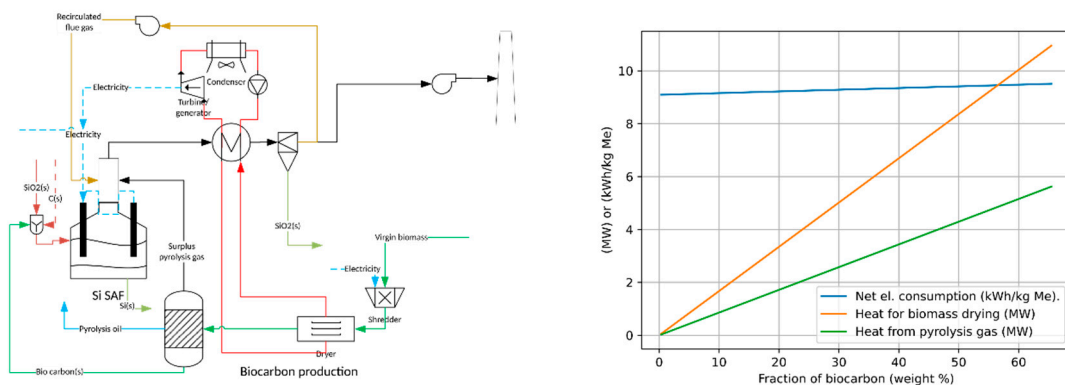
the ferrosilicon production, the use of biocarbon is also relevant for the ferromanganese production in Mo industrial park.



(a) Base case for FeSi production with waste heat recovery and optional use of recirculated flue gas for temperature control. (b) Effect of recirculated flue gas for temperature control in a semi-closed submerged arch furnace (SAF).

Figure 8. FeSi production—base case. Semi-closed furnace with and without recirculated flue gas. See Tables 2 and 3 for design parameters.

Figure 9a shows the base case ferrosilicon process integrated with biocarbon production. Steam from the waste heat recovery boiler is used for the drying of virgin biomass prior to a pyrolysis process for production of biocarbon. By-products from the biocarbon production process are pyrolysis oils and pyrolysis gas. The latter is assumed to be used directly as a heat source and added as hot (combusted) flue gas to the waste heat recovery boiler. The pyrolysis oil has not been included in the energy or CO₂ balance. One may envisage upgrading the pyrolysis oils to more valuable chemicals or fuels as indicated in Figure 7. However, a pragmatic approach has recently been proposed [52] where the pyrolysis oil may be used as binder for the biocarbon material, in which case it would enter the SAF together with the biocarbon and contribute to the waste heat energy production.



(a) Base case FeSi w/biocarbon production. (b) Bio to fossil -carbon ratio - impact on electricity production.

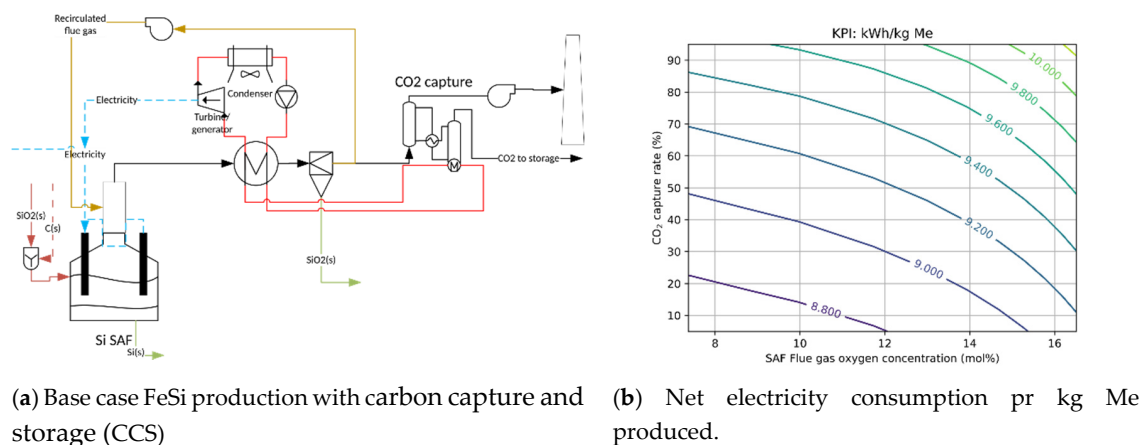
Figure 9. FeSi production with biocarbon. See Tables 2 and 3 for design parameters.

Figure 9b shows the impact of the biocarbon production (given as the bio to fossil carbon ratio) on electricity production, thermal energy consumption for virgin biomass drying and the thermal energy contribution from pyrolysis gas. The increase in net electricity consumption is moderate (~5%) at 70% bio to fossil shares. This is due to the thermal contribution from burning pyrolysis gas generated in the biocarbon production. This makes up for more than 50% of the energy consumed by the drying of virgin biomass.

3.1.3. CO₂ Capture

Carbon capture and storage (CCS) is an alternative or supplement to biocarbon production in order for the ferroalloy production to reduce its carbon footprint. Conventional CO₂ capture is carried out using absorption technology where the regeneration of the solvent (usually amine based) takes place in a stripping column which is operated on thermal energy at around 200 °C. This energy demand is well suited for integration with the steam production in a waste heat recovery unit.

Figure 10a shows the base case FeSi process integrated with an absorption-based CO₂ capture processing unit. The solvent regeneration in the stripper column is operated using steam from the waste heat recovery unit. As with all CO₂ capture technologies, the specific energy demand is linked to the CO₂ concentration in the flue gas through the ideal work of separation (see Figure 5 and [40]). In general, the specific energy demand (MJ/kg CO₂ captured) is reduced with increasing CO₂ concentration. As already demonstrated for the base case (see Figure 8b), a semi-closed SAF will deliver a flue gas with significantly higher concentration (12–14 vol% CO₂) as opposed to around 4 vol% CO₂ in a SAF operating with excess ingress air for temperature control. It is therefore relevant to investigate the impact of both CO₂ capture rate and the oxygen concentration in the flue gas leaving the SAF flue gas combustion zone.



(a) Base case FeSi production with carbon capture and storage (CCS) (b) Net electricity consumption per kg Me produced.

Figure 10. FeSi production integrated with CO₂ capture process. See Tables 2 and 3 for design parameters.

The net electricity consumption in Figure 10b is affected by both the capture rate and the oxygen concentration in the flue gas leaving the SAF combustion zone. This is because the energy demand in the CO₂ capture unit is linked to the CO₂ concentration in the flue gas (see Figure 5). The higher the CO₂ concentration in the flue gas, the less energy has to be provided by the waste heat recovery unit and more electricity can be produced. This is accomplished using a semi-closed SAF operating with low surplus oxygen content and therefore a high CO₂ concentration in the flue gas. According to Figure 10b, a semi-closed furnace with recirculated flue gas for temperature control can achieve almost the same net electricity consumption with 90% carbon capture as a semi-closed furnace operating with ingress air for temperature control and without carbon capture.

3.1.4. Tradeoffs between Biocarbon Production and CO₂ Capture

Exploring the integration between waste heat recovery for electricity production, biocarbon production and CO₂ capture is illustrated in Figure 11a. In the parametric studies illustrated in Figure 11b–d, the key performance indicators are presented as contour lines with biocarbon fraction as the abscissa and CO₂ capture rate as the ordinate. Figure 11b shows that carbon neutral metal production can be achieved with a biocarbon fraction above 55% and 90% capture rate. The associated increased net electricity demand is a 12% increase compared to the lower left corner of Figure 11c.

In terms of the estimated electricity and CO₂ related operating costs in Figure 11d, there is an apparent 40% reduction when moving towards the carbon neutral upper right corner. It is important to notice that the cost figures do not include capital costs associated with any of the proposed measures for increased energy recovery through electricity production, carbon capture or biocarbon production.

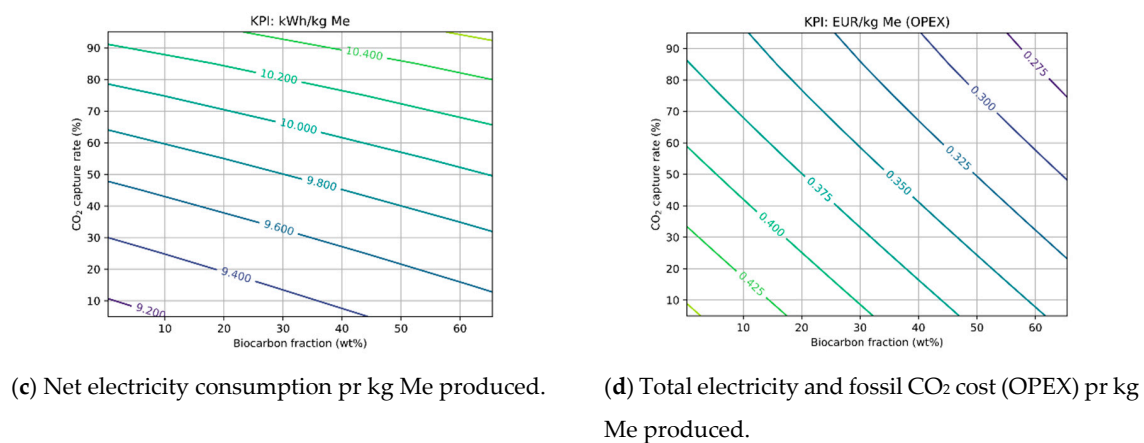
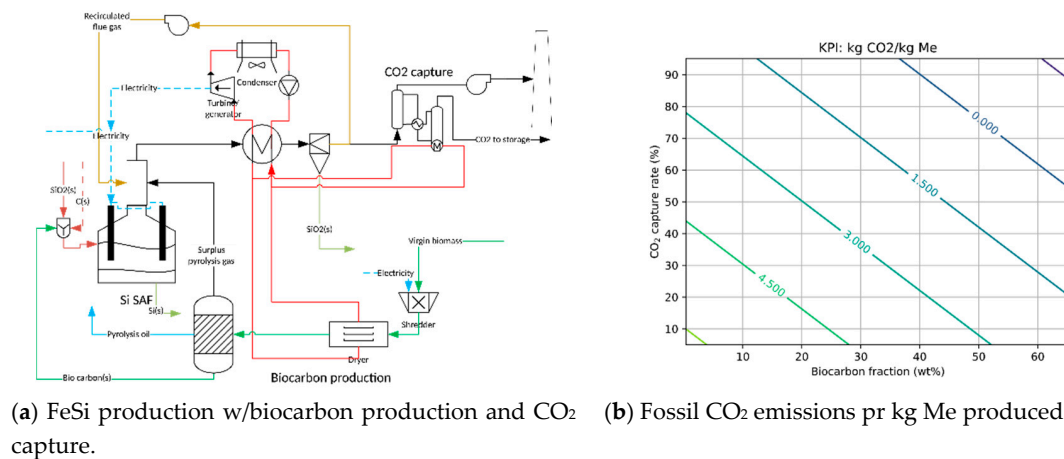


Figure 11. FeSi production with integrated CO₂ capture and biocarbon production. See Tables 2 and 3 for design parameters.

4. Conclusions

The potential for increased energy utilisation and reduced carbon footprint at the Norwegian industry cluster Mo Industri Park has been investigated. Process data on energy flows between the industrial clients in the park show that there is a significant potential for increasing the annual energy recovery within the park. The goal formulated by MIP of increasing the current annual energy recovery of 400 GWh to up to 640 GWh seems technically realistic. This can be accomplished by introducing carbon emission mitigating technologies like carbon capture from flue gas sources within the park and local biocarbon production as a replacement for fossil fuel-based reduction materials in the ferrosilicon production. Both of these measures can, together with conventional electricity production from waste heat recovery units, meet the stated target of energy recovery and at the same time provide close to carbon neutral ferrosilicon production.

The calculations indicate that a semi-closed SAF with recirculated flue gas for temperature control will achieve a 5% lower net electricity consumption compared to a similar SAF using ingress air for temperature control. Further, implementation of recirculation of flue gas will increase the CO₂ concentration and, as a result, decrease the energy demand related to carbon capture. A further

improvement of the energy recovery may be possible if the waste recovery system would be rebuilt to handle higher temperatures, however, this may increase scaling and material wear.

The viability of the biocarbon production will be dependent on the market conditions and the biocarbon price. Establishment of the energy cost for biocarbon from a possible future local biocarbon production should be evaluated in future works to get a more complete picture of the energy input costs.

The current work does not consider that capital costs of implementing the proposed measures and is focused primarily on the ferrosilicon production within the park. This is because the major surplus heat source was associated with flue gas from the ferrosilicon production. However, the proposed measures for energy recovery and carbon emission mitigation are also applicable to the ferromanganese production and to the steel production. In order to carry out a more extensive optimisation of surplus heat utilisation within the park, the utility systems for energy distribution should be considered.

Author Contributions: Conceptualisation, T.P., E.D., P.A.E. and O.T.B.; methodology, T.P.; software, T.P. and E.D.; validation, E.D. and P.A.E.; formal analysis, T.P. and E.D.; investigation, E.D.; resources, E.D.; data curation, E.D.; writing—original draft preparation, T.P., E.D. and P.A.E.; writing—review and editing, O.T.B.; visualisation, E.D.; supervision, O.T.B.; project administration, O.T.B.; funding acquisition, O.T.B. All authors have read and agreed to the published version of the manuscript.

Funding: This publication has been funded by HighEFF—Centre for an Energy Efficient and Competitive Industry for the Future, an eight-year research centre under the FME-scheme (Centre for Environment-friendly Energy Research, 257632/E20). The authors gratefully acknowledge the financial support from the Research Council of Norway and user partners of HighEFF.

Conflicts of Interest: The authors declare no conflict of interest.

Abbreviations

The following abbreviations are used in this manuscript:

CCS	Carbon capture and storage
FeMn	Ferromanganeses production
FeSi	Ferrosilicon production
KPI	Key performance indicator
MEA	Monoethanolamine
MIP	Mo industrial park
SAF	Submerged arch furnace
SRD	Specific reboiler duty (for regeneration of CO ₂ absorbent)

Appendix A. Stream Data for MIP

Tables A1 and A2 show stream data which has been the basis for the grand composite curves for current base case at MIP and for a revised situation with biocarbon production and carbon capture integrated at MIP.

Table A1. Base case stream data as basis for Grand Composite curve in Figure 4.

Process Stream	Tstart (°C)	Tend (°C)	kW/C	MW	GWh
Aga-Heat loss	50	5	111	5	39
BitFury-Heat loss to air	70	5	683	44	350
Celsa-Off gas	250	25	63	14	112
Celsa-Cooling water	10	20	3439	−34	−271
Celsa-Heat loss: Solids& Gas	250	5	80	20	154
Elkem-Mo Fjernvarme: Off gas to district heating	350	180	81	14	108
Elkem-Off gas pipe loss: Flue gas	600	350	168	42	332
Elkem-Off gas cooling:	350	180	88	15	118
Elkem-Off gas, unavoidable heat loss:	180	5	149	26	206
Elkem-Cooling water	5	45	699	−28	−220
Elkem-Heat loss	350	5	50	17	136
Ferroglobe-Heat in solids	1200	5	31	37	291
Ferroglobe-Cooling water	5	45	88	−4	−28
Ferroglobe-Heat loss	200	60	130	18	144

Table A1. Cont.

Process Stream	Tstart (°C)	Tend (°C)	kW/C	MW	GWh
Mo Fjernvarme-Elkem	70	95	548	-14	-108
Mo Fjernvarme-Heat loss: Disposed heat	95	5	49	4	35
Mo Fjernvarme-Heat loss	95	5	9	1	7
Ranfjord fisk-Cooling water	5	16	404	-4	-35
MIP CO distribution network-Heat loss	60	5	64	4	28

Table A2. Revised (Table A1) stream data including proposed future CCS, biocarbon and heat-to-electricity installations at Elkem.

Process Stream	Tstart (°C)	Tend (°C)	kW/C	MW	GWh
Aga-Heat loss	50	5	111	5	39
BitFury-Heat loss	70	5	683	44	350
Celsa-Off gas	250	25	63	14	112
Celsa-Cooling water	10	20	3439	-34	-271
Celsa-Heat loss: Solids& Gas	250	5	80	20	154
Elkem-Mo Fjernvarme: Off gas to district heating	350	180	81	14	108
Elkem-Waste heat recovery: Flue gas	600	350	168	42	332
Elkem-Waste heat recovery	350	180	88	15	118
Elkem-Off gas, unavoidable heat loss	180	5	149	26	206
Elkem-Cooling water	5	45	699	-28	-220
Elkem-Heat loss	350	5	50	17	136
Ferroglobe-Heat in solids	1200	5	31	37	291
Ferroglobe-Cooling water	5	45	88	-4	-28
Ferroglobe-Heat loss	200	60	130	18	144
Mo Fjernvarme-Elkem	70	95	548	-14	-108
Mo Fjernvarme-Heat loss: Disposed heat	95	5	49	4	35
Mo Fjernvarme-Heat loss	95	5	9	1	7
Ranfjord fisk-Cooling water	45	5	111	4	35
MIP CO distribution network-Heat loss	60	5	64	4	28
Elkem-CCS	150	250	260	-28	-221
Elkem-Biocarbon	150	250	80	-14	-110
Elkem-Heat to electricity	45	420	-13.5	-106	

Table A3. Aggregated data on energy flows between companies within MIP. This table is the basis for construction of Sankey diagrams in Figure 3 (excluding the bottom three rows).

Source	Target	Energy Flow (GWh)
Electricity	Aga	50
Aga	Refrigerated product	11
Aga	Heat loss	39
Electricity	BitFury	350
BitFury	Heat loss	350
Electricity	Celsa	352
Coal/Char/Coke	Celsa	49
Gas/oil	Celsa	54
MIP CO nettverk	Celsa	84
Celsa	Off gas	112
Celsa	Cooling water	271
Celsa	Heat loss	154
Electricity	Elkem	785
Coal/Char/Coke	Elkem	860
Biocarbon (current)	Elkem	49
Gas/oil	Elkem	2
Elkem	Mo Fjernvarme	108
Elkem	Waste heat recovery	332
Elkem	Waste heat recovery	118
Elkem	Off gas, unavoidable heat loss	206
Elkem	Chemical energy in product	576

Table A3. Cont.

Source	Target	Energy Flow (GWh)
Elkem	Cooling water	220
Elkem	Heat loss	136
Electricity	Ferroglobe	521
Coal/Char/Coke	Ferroglobe	599
Ferroglobe	MIP CO nettverk	174
Ferroglobe	MIP CO nettverk	174
Ferroglobe	Chemical energy in product	483
Ferroglobe	Heat in solids	291
Ferroglobe	Cooling water	28
Ferroglobe	Heat loss	144
Electricity	Mo Fjernvarme	3
Elkem	Mo Fjernvarme	108
MIP CO nettverk	Mo Fjernvarme	8
Gas/oil	Mo Fjernvarme	6
Mo Fjernvarme	District heating	83
Mo Fjernvarme	Heat loss	35
Mo Fjernvarme	Heat loss	7
Elkem	Cooling water	220
Cooling water	Ranfjord fisk	35
Cooling water	Heat loss	484
Electricity	Ranfjord fisk	5
Cooling water	Ranfjord fisk	35
Ranfjord fisk	Heat loss	40
Ferroglobe	MIP CO nettverk	174
MIP CO nettverk	Celsa	84
MIP CO nettverk	Mo Fjernvarme	8
MIP CO nettverk	SMA Minerals	42
MIP CO nettverk	CO Fakling MIP	42
Heat	MIP CO nettverk	28
MIP CO nettverk	Heat loss	28
Electricity	SMA Minerals	5
MIP CO nettverk	SMA Minerals	42
SMA Minerals	Heat loss	46
Elkem	Waste heat recovery	332
Elkem	Waste heat recovery	118
Waste heat recovery	Biocarbon Production	110
Waste heat recovery	Carbon capture	221
Waste heat recovery	Electricity out	21
Waste heat recovery	Heat loss	97
Biomass	Biocarbon Production	231
Biocarbon Production	Biocarbon	146
Biocarbon Production	Bio oil	81
Waste heat recovery	Biocarbon Production	110
Biocarbon Production	Heat loss	114
Electricity	Carbon capture	30
Waste heat recovery	Carbon capture	221
Carbon capture	Heat loss	251

Appendix B. Quantifying the Surplus Heat

This section will document the data used for establishing the surplus heat flows across battery limits at Mo Industrial Park.

Appendix B.1. General Assumptions

Table A4 lists the estimated energy content of carriers to the companies located within MIP.

Table A4. Energy content of carriers to the industry located within Mo Industrial park.

Energy Carrier	Heating Value (MJ/kg) [53]
Diesel	45.6
Electrode mass	26.0
Anthracite (coal)	32.5
Coke	26.0
Petroleum coke	31.3
Propane	50.4
CO	10.1
Light fuel oil	44.0
Residual oil	39.5
Biocarbon	29.6
Hydrogen	120

Appendix B.2. Celsa

The Celsa facility consists of a steel mill and a rolling mill, which are not co-located in the industrial park. To quantify in what form and quantities the energy leaves Celsa's premises, estimations and assumptions were done for the steel and rolling mill.

The electricity and primary energy consumption were found using data from Norwegian Environment Agency, which provides an important basis for the overall energy basis for Celsa. The data is aggregated to company level, thus not showing the energy use in the steel and rolling mill specifically. Specific heating values were assumed for the energy carriers reported in the mass unit.

It was assumed that all electricity, electrode mass and anthracite were used in the steel mill. With this assumption, the steel mill consumes approximately 75% of the total energy input.

The remaining 25% was allocated to the rolling mill, including the energy carriers CO-rich off-gas from Ferroglobe, light fuel oil, propane and spill oil.

A simplification was assumed that there was no net change in the chemically bound energy in the metal (scrap metal in and metal out). That means all of the energy input is assumed to be transferred to surplus heat.

It was assumed that 30 GWh heat is transferred from the steel mill to the rolling mill by Celsa's internal energy recovery by hot charging [54].

According to Celsa's environmental report, they have an annual cooling water consumption of about 23.3 million m³. Assuming a ΔT of 10 °C, this corresponds to about 271 GWh/year. The cooling water was allocated to the steel and rolling mill with respect to the assumed energy consumption in the two different mills (75%/25%, correspondingly).

The energy in the off-gas from the steel mill was approximated by an energy analysis of a steel mill in the literature [55]. The energy flows from the literature were upscaled linearly by the steel production. This approach yielded an approximated 63 GWh heat in the off-gas from the steel mill.

The energy balance for the steel mill then resulted in an approximate heat loss of 105 GWh/year.

There was not enough information available to quantify the heat in the off-gas from the rolling mill, but it was assumed that 50% of the unaccounted energy (input-known output = unaccounted energy) were losses and 50% was released as off-gas. That corresponds to 50 GWh losses and 50 GWh heat in off-gas.

Appendix B.3. Elkem

The electricity and primary energy consumption were found using data from the Norwegian Environment Agency, which provides an important basis for the overall energy basis for Elkem.

In total, 34% of energy input was assumed to be bound as chemical energy in the product [30], 13% of energy input was assumed transferred to cooling water [30] and 45% of the energy input was assumed to enter the off-gas system [30]. Some of the waste heat of the off-gas is converted to district

heat in the boilers which are connected to the off-gas channels. After the off-gas has passed through the boilers, bag-house filters clean the off-gas from SiO₂ (microsilica), which is a valuable by-product. The temperature at the inlet to the baghouse filters needs to be below 220 and be above 150 °C to avoid corrosion problems [56,57]. The inlet temperature to the district heating boilers were assumed to be 350 °C [58]. It was assumed that the off-gas in practice is utilisable at a temperature level of 600 °C [59]. Based on the assumed temperature levels, the off-gas stream was split into utilisable, already utilised and unavoidable losses.

The remaining 8% was assumed to be heat losses [30].

Appendix B.4. Ferroglobe

The electricity and primary energy consumption were found using data from the Norwegian Environment Agency, which provides an important basis for the overall energy basis for Ferroglobe. An energy analysis of FeMn and SiMn production was used to establish the energy flows leaving the system [60]. Since the specific energy use and metalurgical reactions are different for ferromanganese and silicomanganese, the annual energy flows were weighted by the production of ferromanganese and silicomanganese in 2017.

The CO-gas production was approximated by [60]. The exported CO-gas accounted for approximately 19% of the energy input. The interconnections with other companies in MIP were established using known consumption at Celsa, SMA and Mo Fjernvarme. The remaining energy balance was allocated to flaring at MIP. The internal consumption of CO-gas at Ferroglobe was accounted for [22], but not included in the analysis (since it was within the battery limits).

The chemical energy in the products was an average 34% of energy input. The thermal energy was in products (7%), slag (7%), and off-gas (2%). The losses are summed to 29% of the energy input.

Appendix B.5. Other Actors

The electricity and primary energy consumption were found using data from the Norwegian Environment Agency [22] and the assumed heating values in A4, which provides an important basis for the overall energy balance for SMA Mineral. All input energy was assumed to be converted to heat loss.

Fjernkontrollen.no [61] provides the energy mix of Mo Fjernvarme. The energy mix of consumed district heating was 81% heat from Elkem Ranas off-gas, 9% CO-rich syngas, 7% oil, 3% flexible electricity (2017 numbers). It was assumed that there were 10% losses (7 GWh). An annual disposal of district heat of 35 GWh was assumed [62].

The electricity use of bitfury was assumed to be 350 GWh [63].

The utilisation of cooling water was assumed to be 35 GWh based on information from MIP [64], minus the estimated electricity and district heating consumption of approximately 10 GWh. The electricity use of Ranfjord fisk was estimated by their annual production: 5.5 million smolt, assuming a specific weight of 100 g and a specific energy use of 9 kWh/kg [65].

The electricity use at Aga is 50 MWh based on an 8 MW cryogenic air separator with annual full-load hours of 6250 h (assumption) [66].

References

1. International Energy Agency (IEA). *Tracking Industry Technical Report*; IEA: Paris, France, 2019.
2. Fishedick, M.; Roy, J.; Abdel-Aziz, A.; Acquaye, A.; Allwood, J.; Ceron, J.; Geng, Y.; Kheshgi, H.; Lanza, A.; Perczyk, D.; et al. Chapter 10: Industry. In *Climate Change 2014: Mitigation of Climate Change. Contribution of Working Group III to the Fifth Assessment Report of the Intergovernmental Panel on Climate Change*; Edenhofer, O., Pichs-Madruga, R., Sokona, Y., Farahani, E., Kadner, S., Seyboth, K., Adler, A., Baum, I., Brunner, S., Eickemeier, P., et al., Eds.; Cambridge University Press: Cambridge, UK; New York, NY, USA, 2014; pp. 138–160. [[CrossRef](#)]

3. Kirchherr, J.; Reike, D.; Hekkert, M. Conceptualizing the circular economy: An analysis of 114 definitions. *Resour. Conserv. Recycl.* **2017**, *127*, 221–232. [[CrossRef](#)]
4. Chertow, M.R. Industrial Symbiosis: Literature and Taxonomy. *Annu. Rev. Energy Environ.* **2000**, *25*, 313–337. [[CrossRef](#)]
5. Guo, Y.; Tian, J.; Chertow, M.; Chen, L. Exploring Greenhouse Gas-Mitigation Strategies in Chinese Eco-Industrial Parks by Targeting Energy Infrastructure Stocks. *J. Ind. Ecol.* **2018**, *22*, 106–120. [[CrossRef](#)]
6. Røyne, F.; Hackl, R.; Ringström, E.; Berlin, J. Environmental Evaluation of Industry Cluster Strategies with a Life Cycle Perspective: Replacing Fossil Feedstock with Forest-Based Feedstock and Increasing Thermal Energy Integration. *J. Ind. Ecol.* **2018**, *22*, 694–705. [[CrossRef](#)]
7. Wu, J.; Wang, R.; Pu, G.; Qi, H. Integrated assessment of exergy, energy and carbon dioxide emissions in an iron and steel industrial network. *Appl. Energy* **2016**, *183*, 430–444. [[CrossRef](#)]
8. Yu, B.; Li, X.; Shi, L.; Qian, Y. Quantifying CO₂ emission reduction from industrial symbiosis in integrated steel mills in China. *J. Clean. Prod.* **2015**, *103*, 801–810. [[CrossRef](#)]
9. Johansson, M.T.; Söderström, M. Options for the Swedish steel industry—Energy efficiency measures and fuel conversion. *Energy* **2011**, *36*, 191–198. [[CrossRef](#)]
10. Park, H.S.; Rene, E.R.; Choi, S.M.; Chiu, A.S. Strategies for sustainable development of industrial park in Ulsan, South Korea—From spontaneous evolution to systematic expansion of industrial symbiosis. *J. Environ. Manag.* **2008**, *87*, 1–13. [[CrossRef](#)]
11. Gibbs, D.; Deutz, P. Reflections on implementing industrial ecology through eco-industrial park development. *J. Clean. Prod.* **2007**, *15*, 1683–1695. [[CrossRef](#)]
12. Mattila, T.; Lehtoranta, S.; Sokka, L.; Melanen, M.; Nissinen, A. Methodological Aspects of Applying Life Cycle Assessment to Industrial Symbioses. *J. Ind. Ecol.* **2012**, *16*, 51–60. [[CrossRef](#)]
13. Saidani, M.; Yannou, B.; Leroy, Y.; Cluzel, F.; Kendall, A. A taxonomy of circular economy indicators. *J. Clean. Prod.* **2019**, *207*, 542–559. [[CrossRef](#)]
14. Chae, S.H.; Kim, S.H.; Yoon, S.G.; Park, S. Optimization of a waste heat utilization network in an eco-industrial park. *Appl. Energy* **2010**, *87*, 1978–1988. [[CrossRef](#)]
15. Buoro, D.; Casisi, M.; De Nardi, A.; Pinamonti, P.; Reini, M. Multicriteria optimization of a distributed energy supply system for an industrial area. *Energy* **2013**, *58*, 128–137. [[CrossRef](#)]
16. Yeo, Z.; Masi, D.; Low, J.S.C.; Ng, Y.T.; Tan, P.S.; Barnes, S. Tools for promoting industrial symbiosis: A systematic review. *J. Ind. Ecol.* **2019**, *23*, 1087–1108. [[CrossRef](#)]
17. Dhole, V.; Linnhoff, B. Total site targets for fuel, co-generation, emissions, and cooling. *Comput. Chem. Eng.* **1993**, *17*, 101–109. [[CrossRef](#)]
18. Linnhoff, B.; Townsend, D.; Hewitt, G.; Thomas, B.; Guy, A.; Marsland, R. *A User Guide on Process Integration for the Efficient Use of Energy*; Institution of Chemical Engineers: Rugby, UK, 1983.
19. Klemeš, J.; Dhole, V.; Raissi, K.; Perry, S.; Puigjaner, L. Targeting and design methodology for reduction of fuel, power and CO₂ on total sites. *Appl. Therm. Eng.* **1997**, *17*, 993–1003. [[CrossRef](#)]
20. Matsuda, K.; Hirochi, Y.; Tatsumi, H.; Shire, T. Applying heat integration total site based pinch technology to a large industrial area in Japan to further improve performance of highly efficient process plants. *Energy* **2009**, *34*, 1687–1692. [[CrossRef](#)]
21. Hackl, R.; Harvey, S.; Andersson, E. *Total Site Analysis (TSA) Stenungsund Technical Report*; Chalmers University of Technology: Gothenburg, Sweden, 2010.
22. Norwegian Environment Agency. The Norwegian PRTR—Industry. 2018. Available online: <https://www.norskeutslipp.no/en/Industrial-activities/?SectorID=600> (accessed on 1 February 2020).
23. Gundersen, T. *A Process Integration PRIMER. IEA Tutorial on Process Integration*; SINTEF Energy Research: Trondheim, Norway, 2000.
24. Børset, M.T.; Wilhelmsen, Ø.; Kjelstrup, S.; Burheim, O.S. Exploring the potential for waste heat recovery during metal casting with thermoelectric generators: On-site experiments and mathematical modeling. *Energy* **2017**, *118*, 865–875. [[CrossRef](#)]
25. Schei, A.; Tuset, J.; Tveit, H. *Production of High Silicon Alloys*; Tapir: Trondheim, Norway, 1997.
26. Tangstad, M. Chapter 6—Ferrosilicon and Silicon Technology. In *Handbook of Ferroalloys*; Gasik, M., Ed.; Butterworth-Heinemann: Oxford, UK, 2013; pp. 179–220. [[CrossRef](#)]
27. Kero, I.; Grådahl, S.; Tranell, G. Airborne Emissions from Si/FeSi Production. *JOM* **2017**, *69*, 365–380. [[CrossRef](#)]

28. Wittgens, B.; Panjwani, B.; Pettersen, T.; Jensen, R.; Ravary, B.; Hjertenes, D.O. SCORE Staged combustion for energy Recovery in Ferro-alloy Industries—Experimental Verification. In Proceedings of the Infacon XV, Cape Town, South Africa, 25–28 February 2018.
29. Pettersen, T.; Wittgens, B.; Berglihn, O.T.; Panjwani, B.; Ravary, B.; Myrhaug, E. Reduced environmental impact and increased energy and material recovery in the ferroalloy industry through staged combustion of flue gas. In Proceedings of the 2018 Sustainable Industrial Processing Summit and Exhibition, Rio de Janeiro, Brasil, 4–7 November 2018; Volume 1, p. 18.
30. Takla, M.; Kamfjord, N.; Tveit, H.; Kjelstrup, S. Energy and exergy analysis of the silicon production process. *Energy* **2013**, *58*, 138–146. [[CrossRef](#)]
31. Ladam, Y.; Tangstad, M.; Ravary, B. Energy mapping of industrial ferroalloy plants. In Proceedings of the Thirteenth International Ferroalloys Congress Efficient technologies in Ferroalloy Industry, Almaty, Kazakhstan, 9–12 June 2013; pp. 919–925.
32. Børset, M.; Kolbeinsen, L.; Tveit, H.; Kjelstrup, S. Exergy based efficiency indicators for the silicon furnace. *Energy* **2015**, *90*, 1916–1921. [[CrossRef](#)]
33. Martin, C.R. *PYroMat—Thermodynamic Properties in Python*; The Pennsylvania State University, Altoona College: Altoona, PA, USA, 2018; version 2.0.10.
34. National Institute of Standards and Technology, US Department of Commerce. NIST Chemistry WebBook. 2018. Available online: <https://webbook.nist.gov/chemistry/> (accessed on 1 February 2020).
35. Chase, M. *NIST-JANAF Thermochemical Tables (Journal of Physical and Chemical Reference Data Monographs)*; American Institute of Physics: College Park, MD, USA, 1998; pp. 1–1951.
36. Romera, J.J.G. IAPWS—Python Library for IAPWS Standard Calculation of Water and Steam Properties. Version 1.5.2; 2017. Available online: <https://pypi.org/project/iapws> (accessed on 1 February 2020).
37. Husebye, J.; Brunsvold, A.L.; Roussanaly, S.; Zhang, X. Techno Economic Evaluation of Amine based CO₂ Capture: Impact of CO₂ Concentration and Steam Supply. *Energy Procedia* **2012**, *23*, 381–390. [[CrossRef](#)]
38. Technology Centre Mongstad. About TCM. 2018. Available online: <http://www.tcmda.com/en/About-TCM/> (accessed on 1 February 2020).
39. Gorset, O.; Knudsen, J.N.; Bade, O.M.; Askestad, I. Results from Testing of Aker Solutions Advanced Amine Solvents at CO₂ Technology Centre Mongstad. *Energy Procedia* **2014**, *63*, 6267–6280. [[CrossRef](#)]
40. McGlashan, N.R.; Marquis, A.J. Availability analysis of post-combustion carbon capture systems: Minimum work input. *Proc. Inst. Mech. Eng. Part C J. Mech. Eng. Sci.* **2007**, *221*, 1057–1065. [[CrossRef](#)]
41. Knudsen, J.N.; Andersen, J.; Jensen, J.N.; Biede, O. Evaluation of process upgrades and novel solvents for the post combustion CO₂ capture process in pilot-scale. *Energy Procedia* **2011**, *4*, 1558–1565. [[CrossRef](#)]
42. Olszewski, M.; Kempegowda, R.S.; Skreiberg, Ø.; Wang, L.; Løvås, T. Techno-Economics of Biocarbon Production Processes under Norwegian Conditions. *Energy Fuels* **2017**, *31*, 14338–14356. [[CrossRef](#)]
43. Neves, D.; Thunman, H.; Matos, A.; Tarelho, L.; Gómez-Barea, A. Characterization and prediction of biomass pyrolysis products. *Prog. Energy Combust. Sci.* **2011**, *37*, 611–630. [[CrossRef](#)]
44. Tranberg, B.; Corradi, O.; Lajoie, B.; Gibon, T.; Staffell, I.; Andresen, G.B. Real-time carbon accounting method for the European electricity markets. *Energy Strat. Rev.* **2019**, *26*, 100367. [[CrossRef](#)]
45. Asplan Viak. Nordisk Strøm Blir Renere. 2016. Available online: <https://www.asplanviak.no/aktuelt/2016/02/03/nordiskstroem-blir-renere/> (accessed on 1 February 2020).
46. Watson, F. Factbox: EU CO₂ Price Hits 11-Year High. 2019. Available online: <https://www.spglobal.com/platts/en/marketinsights/latest-news/electric-power/071119-factbox-eu-co2-price-hits-11-year-high> (accessed on 1 February 2020).
47. Eurostat. Electricity Price Statistics. 2019. Available online: https://ec.europa.eu/eurostat/statistics-explained/index.php?title=Electricity_price_statistics#Electricity_prices_for_non-household_consumers (accessed on 1 February 2020).
48. Statistics Norway. Electricity Prices. 2019. Available online: <https://www.ssb.no/energi-og-industri/statistikker/elkraftpris/kvartal/> (accessed on 1 February 2020).
49. Valero Capilla, A.; Valero Delgado, A. *Thanatia: The Destiny of the Earth's Mineral Resources. A Thermodynamic Cradle-to-cradle Assessment*; World Scientific: Singapore, 2014.
50. Magnanelli, E.; Berglihn, O.T.; Kjelstrup, S. Exergy-Based Performance Indicators for Industrial Practice. *Int. J. Energy Res.* **2018**, *42*, 3989–4007. Available online: <https://onlinelibrary.wiley.com/doi/pdf/10.1002/er.4123> (accessed on 1 February 2020). [[CrossRef](#)]

51. Monsen, B.; Grønli, M.; Nygaard, L.; Tveit, H. The Use of Biocarbon in Norwegian Ferroalloy Production. In Proceedings of the INFACON IX, Quebec City, QC, Canada, 3–6 June 2001; Volume 10, p. 10.
52. Riva, L.; Nielsen, H.K.; Skreiberg, Ø.; Wang, L.; Bartocci, P.; Barbanera, M.; Bidini, G.; Fantozzi, F. Analysis of optimal temperature, pressure and binder quantity for the production of biocarbon pellet to be used as a substitute for coke. *Appl. Energy* **2019**, *256*, 113933. [CrossRef]
53. Engineering Toolbox. Fuels—Higher and Lower Calorific Values. 2003. Available online: https://www.engineeringtoolbox.com/fuels-higher-calorific-values-d_169.html (accessed on 1 February 2020).
54. MIP. Celsas Hot Charging Ready for Start Up. 2015. Available online: <https://www.mip.no/en/2015/celsas-hot-charging-ready-for-start-up/> (accessed on 1 February 2020).
55. Tunc, M.; Camdali, U.; Arasil, G. Energy Analysis of the Operation of an Electric-Arc Furnace at a Steel Company in Turkey. *Metallurgist* **2015**, *59*, 489–497. [CrossRef]
56. Hjartarson, H. Waste Heat Utilization at Elkem Ferrosilicon Plant in Iceland. Master's Thesis, University of Iceland, Reykjavík, Iceland, 2009.
57. Kolbeinsen, L.; Lindstad, T.; Tveit, H.; Bruno, M.; Nygaard, L. Energy Recovery in the Norwegian Ferro Alloy Industry. In Proceedings of the INFACON 7, Trondheim, Norway, 11–14 June 1995; pp. 165–177.
58. MIP. Kraft i Bruk fra Vann til Verk. 2012. Available online: <https://www.mip.no/2012/kraft-i-bruk-fra-vann-til-verk/> (accessed on 1 February 2020).
59. Enova. Mo Industripark: Grønn Industriklynge Med Verdensambisjoner. 2017. Available online: <https://www.enova.no/bedrift/industri-og-anlegg/historier/mo-industripark-gronn-industriklynge-med-verdensambisjoner/> (accessed on 1 February 2020).
60. Larsen, T.A.; Tangstad, M.; Kero, I. Energy Distribution in HC FeMn and SiMn—Energy vs. Exergy Analyses. In Proceedings of the Infacon XV, Cape Town, South Africa, 25–28 February 2018.
61. Norsk Fjernvarme. Mo i Rana. 2019. Available online: <https://www.fjernkontrollen.no/mo-i-rana/> (accessed on 1 February 2020).
62. Norsk Fjernvarme. Dumper Spillvarme Påhavet. 2019. Available online: <http://fjernvarmedagene.no/index.php?pageID=29&openLevel=4&cid=4395> (accessed on 1 February 2020).
63. Helgeland Kraft. Helgeland Kraft Inngår Kraftavtale med Norges Største Datasenter. 2019. Available online: <https://www.helgelandkraft.no/konsern/forside/om-helgeland-kraft/nyheter-og-aktuelt/bitfury/> (accessed on 1 February 2020).
64. Ulriksen, A.; Gabor, J. Mo Industrial Park. 2017. Available online: <https://industriysummit.fi/wp-content/uploads/2017/10/Susanne-M.-Naevermo-Sand.pdf> (accessed on 1 February 2020).
65. Bjørndal, T.; Holte, E.A.; Hilmarsen, O.; Tusvik, A. *Analyse av Lukka Oppdrett av Laks-Landbasert og I sjø: Produksjon, Økonomi og Risiko. Technical Report*; NTNU, SINTEF, SNF: Trondheim, Norway, September 2018.
66. MIP. Lindegruppens Nordligste Luftgassfabrikk. 2014. Available online: <https://www.mip.no/2014/lindegruppens-nordligste566luftgassfabrikk/> (accessed on 1 February 2020).

